THE JOURNAL OF PHYSICAL CHEMISTRY A

Article

pubs.acs.org/JPCA

Structural and Electronic Properties of $TM_n[(BN)_3H_6]_m$ Complexes with TM = Co (n, m = 1−3) and with TM = Fe, Ni, Ru, Rh, Pd (n = m = 1−3)

F. Aguilera-Granja,[†] R. H. Aguilera-del-Toro,[†] A. Vega,[‡] and L. C. Balbás*[,‡]

[†]Instituto de Física, Universidad Autónoma de San Luis Potosí, San Luis Potosí, México

[‡]Departamento de Física Teórica, Universidad de Valladolid, 47011 Valladolid, Spain

ABSTRACT: Using the density functional method with the generalized gradient approximation for the exchange and correlation, we investigated the geometrical and electronic properties of free-standing complexes of Co_n clusters combined with hydrogen-saturated boron−nitrogen (BN) rings $[(BN)_3H_6]_m$. The Co atoms tend to form a subcluster capped by BN rings that preserve the Co subcluster against the environment and with which they weakly interact. Thus, the Co subcluster is capable of sustaining a noticeable magnetic moment. These facts are relevant for designing grains with localized magnetic moments. We also optimized those $TM_n[(BN)_3H_6]_n$ complexes with n = 1−3 and TM = Fe, Ni, Ru, Rh, and Pd, starting with the ground-state geometry obtained previously for TM = Co, in order to analyze the dependence of the electronic properties with the number of d electrons in the transition-metal atoms.

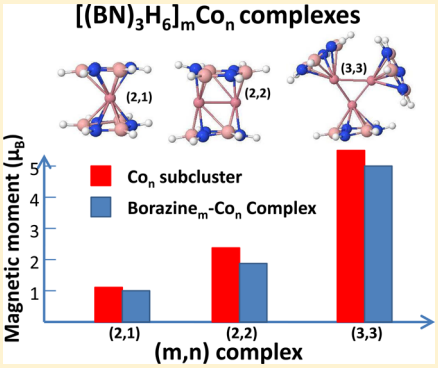

1. INTRODUCTION

Complexes formed by one or several benzene (Bz) rings and transition-metal (TM) atoms have attracted much attention due to their structural and electronic properties and potential technological applications.[1−30] Most of the studies have been focused on the early 3d TM atoms. The strong covalent bond characteristic of the Bz may allow one to preserve its identity, as well as that of the TM atom or subcluster within the complex. This fact facilitates the appearance of localized magnetic moments or indirect magnetic exchange couplings if linear multidecker sandwich structures are stabilized. Half-metallic ferromagnetism[20] or spin transport properties[21] are some examples of electronic properties of interest reported for these systems. From the fundamental viewpoint, understanding the bonding between the Bz and the TM atom or subcluster is of great interest for a better understanding of the structural and electronic properties of extended counterparts like graphene or graphene nanoribbons bearing adsorbed TM impurities.

Regarding the late TM atoms and, in particular Co, stable Co_nBz_m complexes have been experimentally found[1,5] for compositions (m,n) = (2,1), (3,2), (3,3), (4,4), (4,5), (4,6), (4,7), (5,8), and (6,9) with sandwiched structures for n = 1−2, m = n + 1, and more compact structures have been found for n ≥ 3. Charging these complexes with one electron favors the sandwiched structures also for n = 3, m = n, n + 1.[11] Measuring the permanent electric dipole moment allows the experimentalists to get insight on the asymmetry of the geometrical structure.[12] Concerning the magnetic nature of these complexes, Stern−Gerlach measurements have found high magnetic moments for n = 2−4 and relatively low moments for n = 4−10.[19] This points to a sandwiched structure for the smaller complexes and a TM core/Bz shell type structure for the larger ones, in which the TM subcluster is highly coordinated, causing a drop in the magnetic moment.

From the theoretical side, complexes formed by Co atoms and H-saturated Bz's have been recently investigated in the framework of density functional theory (DFT).[27,28] These works have confirmed sandwiched structures for the complexes (1,2), (2,2), and (2,3) and rice-ball structures for (3,3), (3,4), and (4,4). The rice-ball structures can be seen as core/shell type arrangements formed by a TM subcluster capped with Bz. Their findings confirm the structural trends experimentally observed. Regarding the magnetic moments, no clear correlation is found between the high (low) moments and sandwich (core/shell) conformations. Otherwise, relevant data concerning binding energies, ionization potentials (IPs), HOMO−LUMO gap, and polarizabilities were also reported.[27,28] Detailed studies of TM_2Bz_3[29] and $TMBz_2$[30] for a TM of the first row of the periodic table have been recently performed.

Honeycomb structures similar to the one of the graphene sheet can be formed by combining some elements of group IV of the periodic table, as well as with one of group III and another from group V. The corresponding two-dimensional structures have been theoretically investigated within DFT; some of them are planar, while others adopt a low-buckled arrangement.[31] For example, the binding of TM atoms with a graphene-like monolayer of silicon, silicene, have been studied

Received: January 7, 2014
Revised: March 21, 2014
Published: March 27, 2014

   dx.doi.org/10.1021/jp500191v | J. Phys. Chem. A 2014, 118, 2976−2983

recently,[32] as well as the properties of silicene after the adsorption of simple metal atoms.[33] Among the possible combinations of III−V elements, one of the most interesting is that formed by boron and nitrogen rings (borazine), which has the highest cohesive energy and highest in-plane stiffness. To the best of our knowledge, complexes comprising H-saturated boron−nitrogen rings $[(BN)_3H_6]$ and TM atoms have not been investigated so far, neither experimentally nor theoretically. These complexes could exist, in view of the stability of the extended BN sheet and of the strength of the covalent bond. Moreover, interesting electronic properties are also expected for these systems in which the mixed composition of the ring is an additional ingredient.

In the present work, we have conducted DFT calculations in order to predict the structural and electronic properties of complexes formed by H-saturated BN rings (or borazine) and Co atoms, $Co_n[(BN)_3H_6]_m$ with $(m,n) = (1,1)$, $(1,2)$, $(2,1)$, $(2,2)$, $(2,3)$, $(3,2)$, and $(3,3)$. For $n = m = 1-3$, we have also performed calculations considering Fe, Ni, Ru, Rh, and Pd as the TM component, starting with the ground-state geometry obtained previously for TM = Co. The geometries, binding energies, magnetic moments, electric dipole moment, IP, and electron affinity (EA) are determined. The results are compared with those reported for their Bz counterparts. Our results indicate that these nanostructures could also be synthesized in future experiments.

The rest of the paper is organized as follows. Computational details are briefly described in section 2, our results are presented and discussed in section 3, and in section 4, we summarize our main conclusions.

2. THEORETICAL METHOD

We performed systematic DFT calculations using the computational package SIESTA, described in detail in ref 34. For the exchange and correlation potential, we used the Perdew−Burke−Ernzerhof form of the generalized gradient approximation.[35] SIESTA employs numerical pseudoatomic orbitals as basis sets to solve the single-particle Kohn−Sham equations. We have done scalar relativistic calculations. The effects of the spin−orbit (SO) interaction have been investigated, at the DFT level, in clusters of a variety of elements.[36,37] The general conclusion is that only for clusters of certain 5d elements like Pt, the SO interaction may be a driving force as regards the structural and magnetic properties. The effects for 3d and even 4d clusters are small, as they are for B and N. The valence states were described using double-ζ doubly polarized basis sets. The atomic cores were described by nonlocal norm-conserving Troullier−Martins pseudopotentials[38] factorized in the Kleinman−Bylander form.[39] The pseudopotentials for H, B, N, and Co were generated using the valence configurations (cutoff radii) $1s^1$ (1.25 au), $2s^22p^1$ (1.70 au), $2s^22p^3$ (1.24 au), and $4s^13d^8$ (2.0 au), respectively. In the calculations, the clusters were placed in a supercell of size $20 \times 20 \times 20$ Å^3, large enough for the interaction between the cluster and its replicas in neighboring cells to be negligible. We consider only the Γ point ($k = 0$) when integrating over the Brillouin zone. The energy cutoff used to define the real space grid for the numerical calculations involving the electron density was 250 Ry. Using a conjugate gradient method,[40] all of the structures were fully relaxed without any geometry or spin constrain until the interatomic forces were smaller than 0.006 eV/Å. For each structural arrangement of neutral and charged TM−borazine complexes, we have performed initially a free-spin calculation. Further, to ensure the lowest-energy magnetic configuration, we have performed additional calculations, fixing the total spin to neighboring values.

It is not expected that van der Waals dispersion forces play a relevant role in the structural and electronic properties of the present systems. These forces have been shown to be of paramount importance, however, for the adsorption properties of hydrogen on metal-doped graphene nanoribbons[41] or inside of porous cage-like silicon materials doped with TM atoms,[42] for example.

3. RESULTS AND DISCUSSION

Preliminary tests. In Table 1, we report pertinent geometrical and electronic properties of the H-saturated single borazine ring in order to benchmark our theoretical approach against all-electron DFT calculations and experimental data[43,46] when available. Our interatomic distances and angles agree rather well with both all-electron calculations and experimental measurements.[43,46] We computed the binding energy as $E_B = E[(BN)_3H_6] - 6E(H) - 3E(B) - 3E(N)$. The IP and EA were calculated as IP $= E[((BN)_3H_6)^+] - E[(BN)_3H_6]$ and EA $= E[(BN)_3H_6] - E[((BN)_3H_6)^-]$, respectively. The binding energy and IP also agree with all-electron calculations. The large E_B and IP obtained indicate the strength of the covalent bonding of this ring, as expected. We note that both theoretical approaches also agree in the fact that this system does not admit an extra electron as a large negative EA is obtained (somewhat larger in SIESTA). This characteristic also appears in certain complexes, as we will discuss later. Overall, the results found for the single borazine ring in comparison with all-electron calculations and experimental data give us confidence in our theoretical approach. For the TM atoms other than Co, details about the pseudopotentials and basis sets used (together with pertinent tests) can be found in our previous work on the pure 13-atom clusters.[47]

Table 1. Geometrical and Electronic Properties of the H-Saturated Single Borazine Ring $(BN)_3H_6$ from Different Theoretical Approaches[a]

	this work	Gaussian 09	
	SIESTA	6-31G(d,p)	experiments[43,46]
	Geometrical Properties		
	Distance (Å)		
BN	1.432	1.431	1.436 ± 0.004
BH	1.218	1.195	1.258 ± 0.020
NH	1.026	1.010	1.050 ± 0.020
	Angle (degrees)		
B(NBN)	115.80	117.10	117.7 ± 2.0
N(BNB)	124.16	122.90	121.1 ± 2.0
	Electronic Properties		
IP(vertical)(eV)	10.20	10.11	
EA(vertical)(eV)	−1.40	−1.03	
E_B(eV)	−4.423	−4.459	

[a]Experimental data are also reported when available.[43,46].

Structural Configurations. As stated before, the $Co_n[C_6H_6]_m$ complexes have already been studied experimentally[11,19] and theoretically.[27−29] Putative lowest-energy configurations and low-energy isomers have been proposed in those works. For the borazine counterparts, we have considered as input all of the structural conformations suggested in those

dx.doi.org/10.1021/jp500191v | J. Phys. Chem. A 2014, 118, 2976−2983

previous studies: half-sandwich, sandwich (in several versions such as perfect, tilted, double, and coaxial), and rice-ball. We have completed the structural search with additional configurations that may exist when two different species (B and N) form the hexagonal rings instead of just one (C) like in the case of the simple Bz rings. All input structures are fully relaxed according to the criteria indicated in section 2.

In Figures 1 and 2, we show the optimized geometrical structure of the rice configuration (putative ground state) and

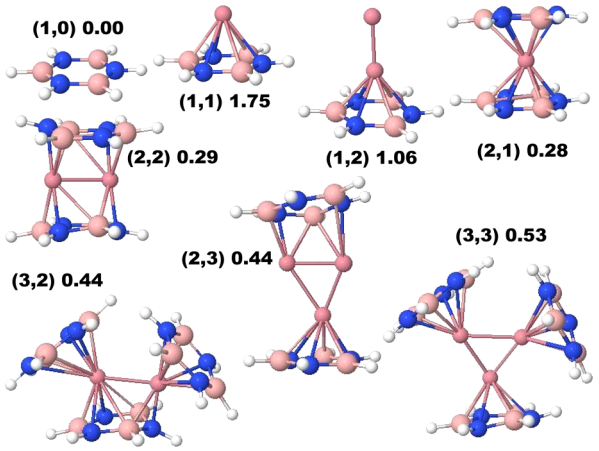

Figure 1. Geometrical structure of the putative ground state of complexes $Co_n[(BN)_3H_6]_m$ with (m,n) = (1,0), (1,1), (1,2), (2,1), (2,2), (2,3), (3,2), and (3,3). For each cluster, identified by the notation (m,n), is given the electric dipole moment in units of Debyes. Red, rose, blue, and gray colors stand for Co, B, N, and H atoms, respectively.

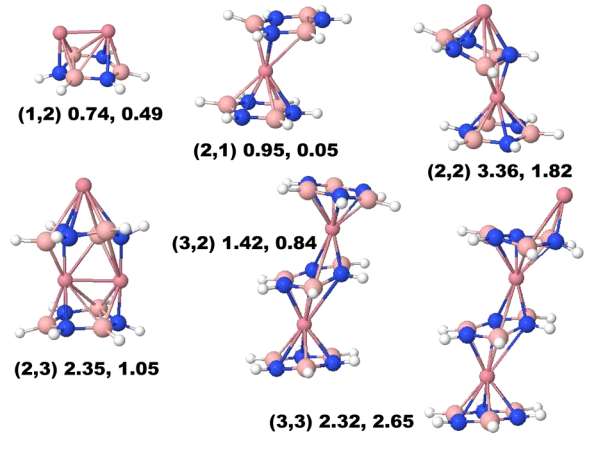

Figure 2. Geometrical structure of the sandwich-like isomers of the complexes $Co_n[(BN)_3H_6]_m$ with (m,n) = (1,2), (2,1), (2,2), (2,3), (3,2), and (3,3). For each cluster, identified by the notation (m,n), is given the electric dipole moment in units of Debyes, and the energy difference, in eV, with respect to the ground state.

sandwich configuration (putative first isomer), respectively, of the different complexes investigated. Tables 2 and 3 report the interatomic distances and characteristic angles of the ground-state structures. We find the following structural trends for the ground state of these complexes: (i) the BN rings retain their identity to a large extent when it comes to comparing interatomic distances and angles (Tables 2 and 3) with those of the free BN ring (Table 1); (ii) the Co atoms form a subcluster, maximizing the number of Co−Co bonds. However,

Table 2. Average Interatomic Distances (in Å) Between the Different Chemical Species in the Ground State of Complexes $Co_n[(BN)_3H_6]_m$, (m,n) = (1,0), (1,1), (1,2), (2,1), (2,2), (2,3), (3,2), and (3,3)[a]

system	BN	NH	BH	CoN	(CoB)	CoCo
(1,0)	1.432	1.026	1.218			
(1,1)	1.448	1.028	1.214	2.421	(2.415)	
(1,2)	1.459	1.027	1.213	2.268	(2.280)	2.108
(2,1)	1.462	1.026	1.213	2.362	(2.242)	
(2,2)	1.473	1.028	1.217	1.982	(2.324)	2.373
(2,3)	1.460	1.028	1.216	2.229	(2.318)	2.281
(3,2)	1.464	1.026	1.212	2.216	(2.277)	2.472
(3,3)	1.457	1.026	1.211	2.293	(2.284)	2.327

[a]The average interatomic distances in the free-standing Co dimer and trimer (triangle) are 2.01 and 2.24 Å, respectively.

Table 3. Average Values of the Characteristic Angles in the Putative Ground State of Complexes $Co_n[(BN)_3H_6]_m$ with (m,n) = (1,0), (1,1), (1,2), (2,1), (2,2), (2,3), (3,2), and (3,3)[a]

System	Angle $\widehat{NBN}$	Angle $\widehat{BNB}$
(1,0)	115.80	124.16
(1,1)	114.63	124.96
(1,2)	114.00	125.73
(2,1)	115.10 (115.10, 115.10)	124.33 (124.33, 124.33)
(2,2)	115.69 (115.67, 115.70)	122.85 (122.77, 122.93)
(2,3)	114.76 (114.00, 115.70)	124.53 (123.40, 125.66)
(3,2)	114.44 (113.23, 114.56, 115.53)	122.98 (120.23, 123.80, 124.93)
(3,3)	114.98 (114.70, 114.90, 115.36)	124.35 (124.07, 124.07, 124.90)

[a]In parentheses are given the values within the different rings of each system.

although the Co subcluster preserves the shape of its free-standing counterpart (dimer for n = 2 and triangle for n = 3), noticeable structural relaxations take place in the presence of the BN rings. Thus, the interatomic distance in the dimer subcluster increases from 2.01 Å in the free-standing environment to 2.37 Å in the complex (2,2) and 2.47 Å in the complex (3,2). Also, the average Co−Co interatomic distance in the trimer subcluster increases from 2.24 Å in the free-standing environment to 2.28 Å in the complex (2,3) and 2.33 Å in the complex (3,3). Therefore, the Co subcluster preserves its identity to a less extent than the BN rings. (iii) The Co subcluster is capped with the H-saturated BN rings to form the (m,n) complexes. This characteristic of the growth pattern is also observed in their counterpart complexes formed by C rings instead of BN rings, although there is an exception.[27] A tilted sandwich structure for the complex formed by three H-saturated C rings and two Co atoms was reported.[27,29] In view of this difference between the (3,2) Bz− and borazine−cobalt complexes, we checked, using the VASP code, that the rice configuration of $Co_2[(BN)_3H_6]_3$ is preferred compared to the sandwich-like one. Another structural difference between our complexes based on BN rings and those based on C rings is that the former adopt, in general, a more symmetrical shape as regards the capping of the Co subcluster with the rings. An example of this fact is the complex (2,1), which is a perfect sandwich (see Figure 1), while its counterpart made of C rings adopts a tilted sandwich configuration[27] in which the Co atom is bonded with all of the C atoms of one ring but only to half of the second. We considered also this possibility and found a somewhat tilted sandwich as the first isomer (see Figure 2). In our case, this loss of symmetry has an energy cost of 50 meV (only 2 meV per atom). The (2,2) complex of BN rings is also

dx.doi.org/10.1021/jp500191v | J. Phys. Chem. A 2014, 118, 2976−2983

more symmetric than its counterpart made of C rings.[27] The reader can find the details concerning interatomic distances and angles in Tables 2 and 3. On the other hand, the dipole moment of compact configurations, that is, those with a compact Co subcluster, is smaller than the one of the sandwich-type isomer, as can be seen comparing the data in Figures 1 and 2. For example, the energy difference between the ground state (rice-like) and the first isomer (sandwich-like) of the (2,3) complex is only 39 meV per atom, but their electric dipole moments are 0.44 and 2.35 D, respectively.

Magnetic Properties. In Figure 3, we plot the total spin magnetic moment of the ground state of $Co_n[(BN)_3H_6]_m$

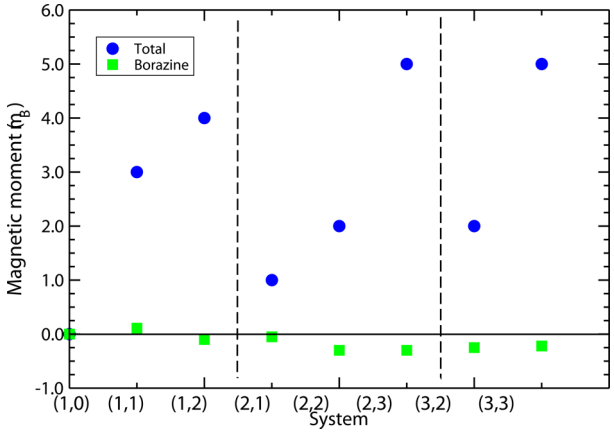

Figure 3. Magnetic properties of the $Co_n[(BN)_3H_6]_m$ complexes as a function of the (m,n) composition. The total magnetic moment (circles) and the one from the rings (squares) are represented.

Table 4. Electronic and Magnetic Properties of the Ground State of $[(BN)_3H_6]_mCo_n$ Complexes[a]

complex (n,m)	$E_B/(12m + n)$ (eV/atom)	$E_{complex}/m$ (eV/m)	VEA (eV)	VIP (eV)	magnetic moment (μ_B)
(1,0)	−4.423	0.0	−1.403	10.197	0.0 (−) P
(1,1)	−4.175	−1.208	0.075	6.255	3.0 (2.89) F
(1,2)	−4.130	−1.223	0.599	7.000	4.0 (4.10) AF
(2,1)	−4.367	−1.519	−0.203	6.412	1.0 (1.05) AF
(2,2)	−4.329	−1.434	0.855	6.156	2.0 (2.30) AF
(2,3)	−4.255	−1.269	1.139	6.117	5.0 (5.30) AF
(3,2)	−4.376	−1.182	0.762	5.721	2.0 (2.25) AF
(3,3)	−4.341	−1.295	1.157	5.857	5.0 (5.22) AF

[a]In the second and third columns are given the binding energy per atom, $E_B/(12m + n)$, and the complex energy per $(BN)_3$ ring, $E_{complex}/m$, respectively. In the fourth and fifth columns are given the vertical electron affinity (VEA) and the vertical ionization potential (VIP), respectively. In the last column, the first number is the total magnetic moment, the number in parentheses is the magnetic moment of the TM subcluster, and the letter describes the magnetic nature of the Borazine rings (P = paramagnetic, F = ferromagnetic, and AF = antiferromagnetic).

complexes (see also the last column of Table 4). As a general trend, noticeable magnetic moments are obtained, up to 5 μ_B in (m,n) = (2,3) and (3,3). The magnetic moment is localized in the Co subcluster, the contribution of the BN ring being negligible and coupled, in general, antiparallel to that of Co. For the $(1,n)$ complexes, with a nonencapsulated Co_n subcluster, the magnetic moment is very close to that of the free-standing Co_n subcluster. The fact that Co atoms tend to form a subcluster favors a parallel magnetic coupling, reminiscent of the ferromagnetic coupling in the Co bulk and, as a consequence, large total moments (although lower than those of the corresponding free-standing Co clusters; we will come later to this point). Therefore, an increase of the total magnetic moment is obtained in (m,n) complexes when increasing the number of Co atoms n. This holds for every value of m (see Figure 3). We note, however, that this increase is not linear. We obtain the same moment (5 μ_B) in (2,3) and (3,3), which have different numbers of BN rings. The same holds for (2,2) and (3,2), which also have different numbers of BN rings and the same moment of 2 μ_B. The two clusters with 5 μ_B have the same Co subcluster (a triangle, apart from slight structural deformations), and the two clusters with 2 μ_B have the same Co subcluster (a dimer). This indicates that the Co subcluster retains a great part of its magnetic properties and that the magnetism of the complex depends more on the size of the Co subcluster than on the number of capping rings. The role played by the capping BN rings on the electronic properties of the Co core deserved to be analyzed in detail. The Co subclusters decrease their magnetic moment (due to the BN capping) as compared to the corresponding free-standing Co clusters. For instance, the Co dimer in the complex (2,2) contributes with 2.30 μ_B to the total moment and with 2.25 μ_B in (3,2), while the relaxed free-standing Co dimer has 4 μ_B. The same holds for the Co trimer, which contributes with 5.30 μ_B in (2,3) and 5.22 μ_B in (3,3), while the relaxed free-standing Co trimer has 7 μ_B. We have seen in the previous subsection that capping the Co subclusters gives rise to a structural expansion, which would tend to increase their moments (in the absence of electronic hybridization with the rings). We observe the opposite behavior. We performed additional calculations of free-standing dimers and trimers with interatomic distances fixed to those in the complexes, and we obtained the same magnetic moments as those of the relaxed free-standing ones. Therefore, we must conclude that the drop in the magnetic moment of the Co subcluster is due to electronic hibridization with the capping BN rings. Nevertheless, we want to stress that they still sustain a noticeable magnetic moment, and what is also important, capping with BN rings preserves them against the environment. Both facts are relevant in the context of the design of grains with localized magnetic moments that possibly should interact with each other through indirect exchange.

For the first isomer of the complexes, those represented in Figure 2, the magnetic moment results in being the same as that for the ground-state structures (compare the last column of Table 4 with that of Table 5). The magnetic moment of the Co_n subcluster in the sandwich-like structures is also nearly the same as that for the ground state.

In Table 6 is given, for the $Co_n-((BN)_3H_6)_m$ complexes studied here, the difference of energy between the ground state of the (m,n) configuration and its spin isomers with a 0−7 μ_B magnetic moment. It can be seen that the minimum energy needed to decrease the spin of the ground-state complex is smaller than that to increase the spin. In addition, for $n \geq 2$, the energy to reach the lower spin state decreases as the number of Borazine units (m) increases. Thus, for very large m, two consecutive spin isomers of a given (m,n) cluster containing the Co_n subcluster can coexist, in principle, at moderate temperature.

dx.doi.org/10.1021/jp500191v | J. Phys. Chem. A 2014, 118, 2976−2983

Table 5. Electronic Properties of the Sandwich-Like Isomer Complexes[a]

complex	$E_B/(12m + n)$ (eV/atom)	$E_{complex}/m$ (eV)	VEA (eV)	VIP (eV)	magnetic moment (μ_B)
(1,2)	−4.095 (0.035)	−0.722	0.485	6.689	4.0 (4.08) AF
(2,1)	−4.365 (0.002)	−1.487	0.393	6.435	1.0 (1.15) AF
(2,2)	−4.259 (0.070)	−2.298	1.162	6.189	2.0 (1.86) F
(2,3)	−4.216 (0.039)	−2.081	1.038	5.867	5.0 (5.17) AF
(3,2)	−4.354 (0.022)	−2.073	0.859	5.698	2.0 (2.26) AF
(3,3)	−4.273 (0.068)	−2.482	1.193	5.784	5.0 (5.13) AF

[a]The entries of the different columns are as those in Table 4. In the second column is also given (in parentheses) the excess energy per atom with respect to the ground state.

Table 6. Energy Difference (in meV per Co atom) of the Magnetic Isomers Having 0−7 μ_B Magnetic Moment with Respect to the Lowest-Energy $[(BN)_3H_6]_mCo_n$ Complex[a]

μ_B (m,n)	0	1	2	3	4	5	6	7
(1,1)	570	85		GS		2797		
(1,2)	1035		500		GS		744	
(2,1)	493	GS		1734		4595		
(2,2)	353		GS		548		1384	
(2,3)	445	293		248		GS		334
(3,2)	276		GS		302		1194	
(3,3)		370		176		GS		548

[a]GS denotes the ground state.

Binding Energy, IP, and EA. We have studied the following electronic descriptors: binding energy (E_B), energy of the complex (E_{com}), vertical ionization potential (VIP), and vertical electron affinity (VEA). The binding energies of the ground-state cluster $Co_n-((BN)_3H_6)_m$ are computed as

$$E_B = E[Co_n - ((BN)_3H_6)_m] - n \times E(Co) - 6 \times m \times E(H) - 3 \times m \times E(B) - 3 \times m \times E(N)$$

The energy of the complex, which describes the stability of the complex with respect to separation of the Co_n subcluster and m borazine units, is computed as

$$E_{complex} = E[Co_n - ((BN)_3H_6)_m] - E[Co_n] - m \times E[(BN)_3H_6]$$

In the case of the sandwich-like configurations, n single atoms are separated by BN rings, so that in the above expression, the term $E[Co_n]$ is substituted by $n \times E(Co)$. For the sandwich (2,3) complex of Figure 2, $E[Co_3]$ is substituted by $E[Co_2] + E(Co)$. The IP of a cluster is the amount of energy required to remove an electron from it. In the case of the clusters $Co_n-((BN)_3H_6)_m$, this quantity is therefore given by

$$IP = E[Co_n - ((BN)_3H_6)_m]^+ - E[Co_n - ((BN)_3H_6)_m]$$

On the other hand, the EA is the energy released when an electron is added to the cluster, that is

$$EA = E[Co_n - ((BN)_3H_6)_m] - E[Co_n - ((BN)_3H_6)_m]^-$$

When no structural relaxation is performed, these quantities are called the VIP and VEA, whereas they are called adiabatic when structural relaxation is taken into account. We report below only results for VIP and VEA. We checked in a few cases that the adiabatic IP and EA values are slightly different compared to the vertical ones.

The binding energy per atom, the complex energy per $(BN)_3H_6$ unit, the vertical EA, the VIP, and the magnetic moment of the Co−borazine complexes are given in Tables 4 and 5 for the ground-state (rice-like) and the first isomer (sandwich-like) configurations, respectively.

In the second column in Table 4 is given the binding energy per atom of the (m,n) borazine complexes in the ground state. For a given $m > 1$, that energy decreases when the size (n) of the Co subcluster increases. Conversely, for a given n, the binding energy increases when the number (m) of $(BN)_3H_6$ rings increases. Thus, the more favorable system results as a balance of the cluster size and the number of $(BN)_3H_6$ layers. On the other hand, the energy for the formation of (m,n) complexes, given in the third column of Table 4, shows a different behavior. For $m = 1$ and 3, it increases when n increases, but for $m = 2$, the complex energy decreases when n increases. However, for a given cluster size, n, there is not an apparent odd−even effect with the number of rings m. Thus, we can not extract a tendency for the relative formation energy of the complexes with their size (m,n).

The VIP of the complexes follows a similar trend to that of the formation energy, but the EA of complexes with fixed m always increases when n increases. Notice that the VEA of the pure $(BN)_3H_6$ ring and of the (2,1) sandwich is negative, that is, the borazine rings (like the Bz rings) are unable to accept one excess electron. This alkaline-earth-like behavior points to a charge transfer from the borazine rings toward the Co atoms.

From the values of the VIP and VEA in Table 5, we can obtain an approximation to the reactivity indexes (IP + EA)/2 (electronegativity) and IP − EA (hardness), assuming that the vertical and adiabatic values are close. The highest electronegativity is obtained for the (1,2) complex formed by an elongated Co_2 dimer capping one borazine ring. For a given m, the IP of the complex correlates with the formation energy. On the other hand, the hardness, IP − EA, is supposed to be a better approximation to the physical HOMO−LUMO gap than the Kohn−Sham gap obtained from the eigenvalues of the HOMO and LUMO orbitals. Using our VIP and VEA values as approximations to the relaxed IP and EA, the largest hardness is obtained for the (2,1) complex. The largest Kohn−Sham gap occurs also for the (2,1) complex (see Table 7), but it is a factor of four smaller than the physical gap.

In Table 5 are given the same magnitudes as those in Table 4, now for the sandwich-like complexes represented in Figure 2. For these structures, there are no changes in the total magnetic moment as compared to that of the rice-like structures, and the magnetic moment of the Co subcluster suffers a minimal variation, except for the (2,2) complex. Also, for the (2,2) case, it is observed that there is a variation in the trends with n of the formation energy and EA of rice-like versus sandwich-like (m,n)

dx.doi.org/10.1021/jp500191v | J. Phys. Chem. A 2014, 118, 2976−2983

Table 7. Khon−Sham HOMO−LUMO Gap (in eV) for the Different Clusters Here Considered

borazine/Co	0	1	2	3
0	0.00	0.03		
1	6.13	0.66	0.83	
2		1.62	0.53	0.44
3			0.98	0.61

structures. The largest difference of electric dipole moment between both structures also occurs at the (2,2) complex.

In Figure 4 are shown the structures of $TM_n-[(BN)_3H_6]_n$ complexes with n = 3 for TM = Fe, Ni, Ru, Rh, and Pd, as

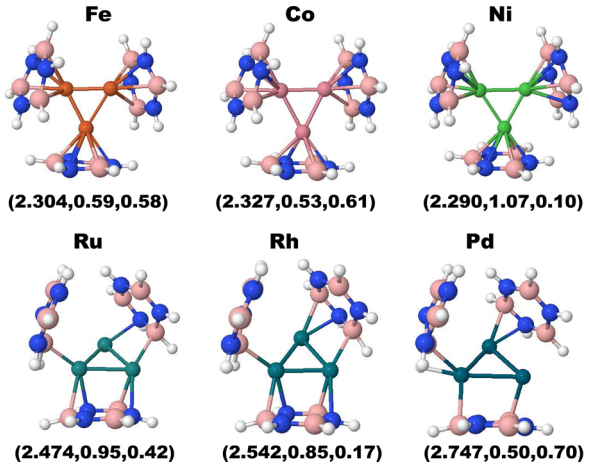

Figure 4. Geometrical structure of $TM_3[(BN)_3H_6]_3$ clusters. In parentheses are shown the TM-distance (Å), electric dipole (Debye), and Kohn−Sham Gap (eV).

optimized starting from the corresponding ground-state structure of the complex with TM = Co. The structures for the smaller sizes are not shown. The average TM−TM distance (in Å), the electric dipole (in Debye), and the Kohn−Sham HOMO−LUMO gap (in eV) are given below each structure. For the 3d complexes, the optimized structure is, for all sizes, similar to that shown for TM = Co in Figure 1. The same holds for the 4d complexes with n = 1,2. However, for the 4d complexes of n = 3, the subcluster TM_n is still embeded in a rice configuration, but the bonding between the TM clusters and borazine rings is different, thus exhibiting a noticeable distortion. Whereas for 3d elements that bonding is hexahapto for each one of the TM atoms, for 4d elements, the bonding is trihapto for two of the TM atoms toward the same borazine ring and is dihapto for the third TM toward another borazine ring, being the third borazine ring linked to one of the former TM atoms. The fact that the 4d (3,3) complexes deform the structure of the analogous complex of Co so much could be due to the larger size of these 4d-TM subclusters compared to that of the Co_3 ones, as can be seen in Table 8. Because we did not perform a structural search as extensive as that of the Co compounds, we cannot exclude the possibility of a more stable structural configuration. In Table 8, it is also apparent that the average TM−TM distance in the subclusters is larger than that in their free-standing counterparts, an exception being Fe.

In Table 9 are given, for $TM_n-[(BN)_3H_6]_n$ complexes (n = 1−3), values obtained for those magnitudes shown in Table 4 for TM = Co. The binding energy per atom seems to be saturated at n = 2, as long as no energy gain results in passing

Table 8. Comparison of the Interatomic Distances (Å) and the Magnetism (μ_B) in the Complex Systems and the Free TM Clusters

	distances		Espin	
properties	complex (•, •−•, Δ)	free (•, •−•, Δ)	complex (•, •−•, Δ)	free (•, •−•, Δ)
TM−Benzine				
Fe (1,2,3)	−, 2.235, 2.304	−, 2.04, 2.317	2, 4, 8	4, 6, 10
Co (1,2,3)	−, 2.373, 2.327	−, 2.02, 2.259	3, 2, 5	3, 4, 7
Ni (1,2,3)	−, 2.516, 2.290	−, 2.17, 2.275	0, 0, 2	2, 2, 2
Ru (1,2,3)	−, 2.276, 2.474	−, 2.08, 2.433	2, 2, 4	4, 4, 8
Rh (1,2,3)	−, 2.581, 2.542	−, 2.27, 2.486	1, 2, 1	3, 4, 5
Pd (1,2,3)	−, 2.837, 2.747	−, 2.52, 2.571	0, 0, 0	0, 1, 2

Table 9. Electronic Properties of $TM_n[(BN)_3H_6]_n$ Complexes (n = 1−3) for TM = Fe, Co, Ni, Ru, Rh, and Pd[a]

system	$E_B/13 \times n$ (eV/atom)	$E_{complex}/n$ (eV)	VEA (eV)	VIP (eV)	magnetic moment (μ_B)
		Fe			
(1,1)	−4.155	−0.945	0.501	6.441	2.00 (2.26) AF
(2,2)	−4.295	−1.196	0.633	5.839	4.00 (4.63) AF
(3,3)	−4.304	−0.928	1.054	5.465	8.00 (8.41) AF
		Co			
(1,1)	−4.175	−1.208	0.075	6.255	3.0 (2.89) F
(2,2)	−4.329	−1.434	0.855	6.156	2.0 (2.30) AF
(3,3)	−4.341	−1.296	1.157	5.857	5.0 (5.22) AF
		Ni			
(1,1)	−4.164	−1.063	0.121	6.893	0.00 (0.00) P
(2,2)	−4.315	−1.680	0.152	6.167	0.00 (0.00) P
(3,3)	−4.307	−1.164	1.269	5.808	2.00 (2.00) P
		Ru			
(1,1)	−4.229	−1.913	0.458	7.329	2.00 (1.93) F
(2,2)	−4.371	−1.607	1.061	6.439	2.00 (2.11) AF
(3,3)	−4.371	−1.015	1.747	6.188	4.00 (4.12) AF
(3,3)*	−4.368	−0.974	1.309	5.781	2.00 (1.79) F
		Rh			
(1,1)	−4.223	−1.821	0.378	6.990	1.00 (0.92) F
(2,2)	−4.360	−1.813	1.434	6.488	2.00 (1.98) F/P
(2,2)*	−4.360	−1.813	1.409	6.540	0.00 (0.00) F/P
(3,3)	−4.363	−1.276	1.811	6.526	1.00 (1.05) AF
		Pd			
(1,1)	−4.165	−1.077	0.268	7.761	0.00 (0.00) P
(2,2)	−4.263	−1.588	0.028	6.521	0.00 (0.00) P
(3,3)	−4.265	−1.068	1.713	6.571	0.00 (0.00) P

[a]The entries of the different columns as those in Table 4.

from n = 2 to 3. The formation energy of the complex, per borazine unit, shows a maximum for the (2,2) complexes, with the exception of TM = Ru, which exhibits a decreasing value when n increases. On the other hand, the hardness (VIP − VEA), which is an approximation to the exact HOMO−LUMO gap, always decreases as n increases. The same fact occurs with the VIP except for Rh and Pd complexes, in which the VIP for n = 2 and 3 reaches nearly the same value.

Concerning the magnetic moments, the TM subcluster contributes to most of the total magnetic moment of the complex, as in the case of TM = Co. A comparison of that value with the one of the free-standing TM subcluster is given in Table 8, where the interatomic TM−TM average distances are also provided. Finally, the type of magnetic coupling of the borazines for each of the studied complexes is also given in

dx.doi.org/10.1021/jp500191v | J. Phys. Chem. A 2014, 118, 2976−2983

Table 9. From our results, Fe is the best TM element to build these compounds as far as the total magnetic moment is concerned. Those made of the 4d elements have lower magnetic moments than their isoelectronic 3d counterparts, the most remarkable case being the one with TM = Pd, which results in being nonmagnetic, independent of the size. However, in the case of Ru and Rh, the magnetic anisotropy is expected to be larger than that in the 3d ones, a fact that might be important for certain applications like magnetic storage.

4. CONCLUSIONS

Our DFT-GGA study of the structural and electronic properties of complexes formed by H-saturated BN rings and Co atoms, $Co_n[(BN)_3H_6]_m$, allows one to infer the following conclusions:

(i) The H-saturated BN rings retain their identity to a large extent, while Co atoms tend to form a compact subcluster capped with those rings.

(ii) Interaction of Co with the BN rings is weak but not negligeable as it results in larger Co−Co interatomic distances and a lower spin magnetic moment in the subcluster than those in its free-standing counterpart despite the larger interatomic distances within the complex.

(iii) The complex sustains a noticeable total magnetic moment, mostly localized in the Co subcluster, that increases as its size increases (for instance, 5 μ_B when the Co subcluster has three atoms).

(iv) For a given $m > 1$, the binding energy decreases when the size (n) of the Co subcluster increases, and vice versa; for a given n, the binding energy increases when the number (m) of $(BN)_3H_6$ rings increases.

(v) When subtituting Co with the other 3d ferromagnetic elements (Fe, Ni) as well as by their isoelectronic 4d (Ru, Rh, Pd) in the putative ground states with $n = m$, we obtain similar structures after relaxation, except for $n = m = 3$ in the case of the 4d subclusters where the complexes are strongly distorted. As a general trend, the 4d complexes have a lower total magnetic moment than the corresponding 3d ones.

Overall, the conclusions drawn in the present study are promising for the design of organometallic nanomagnets, able to sustain a net magnetic moment, localized and preserved against environmental agents. Further investigation in this line concerning 5d elements and bimetallic 3d−5d subclusters would be also appealing because the resulting complexes could also have a large magnetic anisotropy together with a noticeable net magnetic moment.[37]

AUTHOR INFORMATION

Corresponding Author

*E-mail: balbas@fta.uva.es.

Notes

The authors declare no competing financial interest.

ACKNOWLEDGMENTS

This work was supported by PROMEP-SEP-CA230, México, and by the Spanish Ministry of Science and Innovation (Project FIS2011-22957) in conjunction with the European Regional Development Fund. F.A-G acknowledges the financial support provided by the University of Valladolid for a research visit. R.H.A-T acknowledges a fellowship from CONACyT. We would like to acknowledge helpful discussions with Prof. Pis-Diez.

REFERENCES

(1) Kurikawa, T.; Hirano, M.; Takeda, H.; Yagi, K.; Hoshino, K.; Nakajima, A.; Kaya, K. Structures and Ionization Energies of Cobalt−Benzene Clusters (Co_n(Benzene)$_m$). *J. Phys. Chem.* **1995**, *99*, 16248−16252.

(2) Meyer, F.; Khan, F. A.; Armentrout, P. B. Thermochemistry of Transition Metal Benzene Complexes: Binding Energies of M-$(C_6H_6)^{x+}$ (x = 1, 2) for M = Ti to Cu. *J. Am. Chem. Soc.* **1995**, *117*, 9740−9748.

(3) Ouhlal, A.; Selmani, A.; Yelon, A. Bonding in (η^6-C_6H_6)M and (η^6-C_6H_6)M$^+$, M = Ti, Cr, Ni, and Cu. A Local Spin Density Study. *Chem. Phys. Lett.* **1995**, *243*, 269−274.

(4) Weis, P.; Kemper, P. R.; Bowers, M. T. Structures and Energetics of $V_n(C_6H_6)^{m+}$ Clusters: Evidence for a Quintuple-Decker Sandwich. *J. Phys. Chem. A* **1997**, *101*, 8207−8213.

(5) Kurikawa, T.; Takeda, H.; Hirano, M.; Judai, K.; Arita, T.; Nagao, S.; Nakajima, A.; Kaya, K. Electronic Properties of Organometallic Metal−Benzene Complexes [M_n(benzene)$_m$ (M = Sc−Cu)]. *Organometallics* **1999**, *18*, 1430−1438.

(6) Yang, C. N.; Klippenstein, S. J. Theory and Modeling of the Binding in Cationic Transition-Metal−Benzene Complexes. *J. Phys. Chem. A* **1999**, *103*, 1094−1103.

(7) Yasuike, T.; Yabushita, S. Ionization Energies and Bonding Scheme of Multiple-Decker Sandwich Clusters: $M_n(C_6H_6)_{n+1}$. *J. Phys. Chem. A* **1999**, *103*, 4533−4542.

(8) Nakajima, A.; Kaya, K. A Novel Network Structure of Organometallic Clusters in the Gas Phase. *J. Phys. Chem. A* **2000**, *104*, 176−191.

(9) Chaquin, P.; Costa, D.; Lepetit, C.; Che, M. Structure and Bonding in a Series of Neutral and Cationic Transition Metal−Benzene η^6 Complexes [M(η^6-C_6H_6)]$^{n+}$ (M = Ti, V, Cr, Fe, Co, Ni, and Cu). Correlation of Charge Transfer with the Bathochromic Shift of the E_1 Ring Vibration. *J. Phys. Chem. A* **2001**, *105*, 4541−4545.

(10) Pandey, R.; Rao, B. K.; Jena, P.; Blanco, M. A. Electronic Structure and Properties of Transition Metal−Benzene Complexes. *J. Am. Chem. Soc.* **2001**, *123*, 3799−3808.

(11) Gerhards, M.; Thomas, O. C.; Nilles, J. M.; Zheng, W. J.; Bowen, K. H., Jr. Cobalt−Benzene Cluster Anions: Mass Spectrometry and Negative Ion Photoelectron Spectroscopy. *J. Chem. Phys.* **2002**, *116*, 10247−10252.

(12) Rayane, D.; Allouche, A. R.; Antoine, R.; Broyer, M.; Compagnon, I.; Dugourd, P. Electric Dipole of Metal−Benzene Sandwiches. *Chem. Phys. Lett.* **2003**, *375*, 506−510.

(13) Jaeger, T. D.; Heijinsbergen, D. V.; Klippenstein, S. J.; Helden, G.; Meijer, G.; Duncan, M. A. Vibrational Spectroscopy and Density Functional Theory of Transition-Metal Ion−Benzene and Dibenzene Complexes in the Gas Phase. *J. Am. Chem. Soc.* **2004**, *126*, 10981−10991.

(14) Miyajima, K.; Nakajima, A.; Yabushita, S.; Knickelbein, M. B.; Kaya, K. Ferromagnetism in One-Dimensional Vanadium−Benzene Sandwich Clusters. *J. Am. Chem. Soc.* **2004**, *126*, 13202−13203.

(15) Wang, J.; Acioli, P. H.; Jellinek, J. Structure and Magnetism of V_nBz_{n+1} Sandwich Clusters. *J. Am. Chem. Soc.* **2005**, *127*, 2812−2813.

(16) Zheng, W. J.; Nilles, J. M.; Thomas, O. C.; Bowen, K. H., Jr. Photoelectron Spectroscopy of Titanium−Benzene Cluster Anions. *Chem. Phys. Lett.* **2005**, *401*, 266−270.

(17) Rabilloud, F. Geometry and Spin-Multiplicity of Half-Sandwich Type Transition-Metal−Benzene Complexes. *J. Chem. Phys.* **2005**, *122*, 134303/1−134303/6.

(18) Sohnlein, B. R.; Li, S. G.; Yang, D. S. Electron-Spin Multiplicities and Molecular Structures of Neutral and Ionic Scandium−Benzene Complexes. *J. Chem. Phys.* **2005**, *123*, 214306/1−214306/7.

(19) Knickelbein, M. B. Magnetic Moments of Bare and Benzene-Capped Cobalt Clusters. *J. Chem. Phys.* **2006**, *125*, 044308/1−044308/7.

(20) Maslyuk, V. V.; Bagrets, A.; Meded, V.; Arnold, A.; Evers, F.; Brandbyge, M.; Bredow, T.; Mertig, I. Organometallic Benzene−

Vanadium Wire: A One-Dimensional Half-Metallic Ferromagnet. *Phys. Rev. Lett.* **2006**, *97*, 097201/1−097201/4.
(21) Xiang, H. J.; Yang, J. L.; Hou, J. G.; Zhu, Q. S. One-Dimensional Transition Metal-Benzene Sandwich Polymers: Possible Ideal Conductors for Spin Transport. *J. Am. Chem. Soc.* **2006**, *128*, 2310−2314.
(22) Bechamp, K.; Levesque, M.; Joly, H.; Manceron, L. A Combined Electron Paramagnetic Resonance and Fourier Transform Infrared Study of the $Co(C_6H_6)_{1,2}$ Complexes Isolated in Neat Benzene or in Cryogenic Matrixes. *J. Phys. Chem. A* **2006**, *110*, 6023−6031.
(23) Zhou, J.; Wang, W. N.; Fan, K. N. Novel Compounds with Cobalt, Copper, and Nickel Dimers Sandwiched between Benzene Molecules: A DFT Study. *Chem. Phys. Lett.* **2006**, *424*, 247−251.
(24) Kua, J.; Tomlin, K. M. Computational Study of Multiple-Decker Sandwich and Rice-Ball Structures of Neutral Titanium−Benzene Clusters. *J. Phys. Chem. A* **2006**, *110*, 11988−11994.
(25) Nagaoka, S.; Matsumoto, T.; Ikemoto, K.; Mitsui, M.; Nakajima, A. Soft-Landing Isolation of Multidecker $V_2(Benzene)_3$ Complexes in an Organic Monolayer Matrix: An Infrared Spectroscopy and Thermal Desorption Study. *J. Am. Chem. Soc.* **2007**, *129*, 1528−1529.
(26) Miyajima, K.; Yabushita, S.; Knickelbein, M. B.; Nakajima, A. Stern−Gerlach Experiments of One-Dimensional Metal−Benzene Sandwich Clusters: $M_n(C_6H_6)_m$ (M = Al, Sc, Ti, and V). *J. Am. Chem. Soc.* **2007**, *129*, 8473−8480.
(27) Zhang, X.; Wang, J. Structural, Electronic, and Magnetic Properties of $Co_n(Benzene)_m$ Complexes. *J. Phys. Chem. A* **2008**, *112*, 296−304.
(28) Wang, J.; Zhu, L.; Zhang, X.; Yang, M. Size- and Shape-Dependent Polarizabilities of Sandwich and Rice-Ball ConBzm Clusters from Density Functional Theory. *J. Phys. Chem. A* **2008**, *112*, 8226−8230.
(29) Liu, H.; Li, Q.-S.; Xie, Y.; Bruce King, R.; Schaefer, H. F., III. Triple-Decker-Sandwich versus Rice-Ball Structures for Tris-(benzene)dimetal Derivatives of the First-Row Transition Metals. *J. Phys. Chem. A* **2011**, *115*, 9022−9032.
(30) Seung Youn, I.; Young Kim, D.; Jiten Singh, N.; Woo Park, S.; Youn, J.; Kim, K. S. Intercalation of Transition Metals into Stacked Benzene Rings: A Model Study of the Intercalation of Transition Metals into Bilayered Graphene. *J. Chem. Theory Comput.* **2012**, *8*, 99−105.
(31) Sahin, H.; Cahangirov, S.; Topsakal, M.; Bekaroglu, E.; Akturk, E.; Senger, R. T.; Ciraci, S. Monolayer Honeycomb Structures of Group-IV Elements and III−V Binary Compounds: First-Principles Calculations. *Phys. Rev. B* **2009**, *80*, 155453/1−155453/12.
(32) Sahin, H.; Peeters, F. M. Adsorption of Alkali, Alkaline-Earth, and 3d Transition Metal Atoms on Silicene. *Phys. Rev. B* **2013**, *87*, 085423/1−085423/9.
(33) Sivek, J.; Sahin, H.; Partoens, B.; Peeters, F. M. Adsorption and Absorption of Boron, Nitrogen, Aluminum, and Phosphorus on Silicene: Stability and Electronic and Phonon Properties. *Phys. Rev. B* **2013**, *87*, 085444/1−085444/8.
(34) Soler, J. M.; Artacho, E.; Gale, J. D.; Garca, A.; Junquera, J.; Ordejon, P.; Sánchez-Portal, D. The SIESTA Method for Ab Initio Order-N Materials Simulation. *J. Phys.: Condens. Matter* **2002**, *14*, 2745−2749.
(35) Perdew, J. P.; Burke, K.; Ernzerhof, M. Generalized Gradient Approximation Made Simple. *Phys. Rev. Lett.* **1996**, *77*, 3865−3868.
(36) Błoński, P.; Hafner, J. Magneto-Structural Properties and Magnetic Anisotropy of Small Transition-Metal Clusters: A First-Principles Study. *J. Phys.: Condens. Matter* **2011**, *23*, 136001/1−136001/19.
(37) Alvarado-Leyva, P. G.; Aguilera-Granja, F.; García-Fuente, A.; Vega, A. Spin Orbit Effects on the Structural, Homotop, and Magnetic Configurations of Small Pure and Fe-Doped Pt Clusters. *J. Nanopart. Res.* **2014**, *16*, 2222/1−2222/11.
(38) Troullier, N.; Martins, J. L. Efficient Pseudopotentials for Plane-Wave Calculations. *Phys. Rev. B* **1991**, *43*, 1993−2006.
(39) Kleinman, L.; Bilander, D. M. Efficacious Form for Model Pseudopotentials. *Phys. Rev. Lett.* **1982**, *48*, 1425−1428.
(40) Press, W. H.; Teukolsky, S. A.; Vetterling, W. T.; Flannery, B. P. *Numerical Recipes in Fortran*, 2nd ed.; Cambridge University Press: Cambridge, U.K., 1992.
(41) Carrete, J.; Longo, R. C.; Gallego, J.; Vega, A.; Balbás, L. C. Al Enhances the H_2 Storage Capacity of Graphene at Nanoribbon Borders but Not at Central Sites. A Study Using Non Local Van Der Waals Density Functionals. *Phys. Rev. B* **2012**, *85*, 125435/1−125435/7.
(42) Cantera, H.; Fernández, E. M.; Balbás, L. C.; Borstel, G. Adsorption of H, H_2, and H_2O Inside and Outside of $(M@Si_{16}F)_6$ Tube-Like Aggregates and Wires (M = V, Ta). A First Principles Study. *Mater. Chem. Phys.* **2013**, *139*, 247−255.
(43) Boyd, R. J.; Choi, S. Ch.; Hale, Ch. C. Electronic and Structural Properties of Borazine and Related Molecules. *Chem. Phys. Lett.* **1984**, *112*, 136−141.
(44) Kresse, G.; Hafner, J. Ab Initio Molecular Dynamics for Liquid Metals. *Phys. Rev. B* **1993**, *47*, 558−561.
(45) Kresse, G.; Furthmüller, J. Efficient Iterative Schemes for Ab Initio Total-Energy Calculations Using a Plane-Wave Basis Set. *Phys. Rev. B* **1996**, *54*, 11169−11186.
(46) Callomon, J. H.; Hirota, E.; Kuchitsu, V.; Lafferty, W. J.; Maki, V.; Pote, C. S. In *Structure Data of Free Polyatomic Molecules*; Hellwege, K. H., Hellwege, A. M., Eds.; Springer: Berlin, Germany, 1976.
(47) Aguilera-Granja, F.; García-Fuente, A.; Vega, A. Comparative Ab Initio Study of the Structural, Electronic, and Magnetic Trends of Isoelectronic Late 3d and 4d Transition Metal Clusters. *Phys. Rev. B* **2008**, *78*, 134425/1−134425/9.